arXiv:cond-mat/0409211v2 [cond-mat.mes-hall] 26 Jul 2005

Mesoscopic Kondo Problem

R. K. KAUL, D. ULLMO, S. CHANDRASEKHARAN and H. U. BARANGER
Department of Physics, Duke University, Durham, NC 27708-0305.

PACS. 73.23.Hk – Coulomb blockade; single-electron tunneling.
PACS. 72.15 Qm – Scattering mechanisms and Kondo effect.
PACS. 73.63.Kv – Semiclassical chaos ("quantum chaos").

Abstract. – We study the effect of mesoscopic fluctuations on a magnetic impurity coupled to a spatially confined electron gas with a temperature in the mesoscopic range (i.e. between the mean level spacing Δ and the Thouless energy $E_{\rm Th}$). Comparing "poor-man's scaling" with exact Quantum Monte Carlo, we find that for temperatures larger than the Kondo temperature, many aspects of the fluctuations can be captured by the perturbative technique. Using this technique in conjunction with semi-classical approximations, we are able to calculate the mesoscopic fluctuations for a wide variety of systems. For temperatures smaller than the Kondo temperature, we find large fluctuations and deviations from the universal behavior.

The nature of many-body interaction effects at the nanoscale has been of great interest recently. Examples include, for instance, charging and correlation in quantum dots [1], superconductivity or ferromagnetism in metallic grains [2], and transport through effectively one-dimensional systems [3]. Since interference effects are ubiquitous at the nanoscale, it is natural to examine the interplay between interference and many-body interactions in these systems.

A magnetic impurity coupled to an electron gas is a classic many-body problem, known as the Kondo problem [4]. In the simplest case, one takes a spin-1/2 impurity coupled antiferromagnetically with an exchange constant J to an electron gas described by a constant density of states ρ_0 within a bandwidth D. The physics has two distinct temperature regimes – at high T the electrons scatter off the impurity in inelastic spin-flip processes, while at low T there is only elastic scattering as the impurity is screened by electrons forming a bound state singlet. The crossover takes place at an energy scale T_K^0, which in the weak coupling limit $\simeq De^{-1/J\rho_0}$. All impurity properties (i.e. impurity contribution to thermodynamic quantities and impurity correlators) have temperature dependencies that are *universal* after rescaling with T_K^0. This simplest case corresponds to a bulk piece of metal in which there is no interference.

More recently, the effect of interference on Kondo impurities has been studied in various open systems. In disordered metals, the presence of magnetic impurities affects the weak-localization properties [5, 6], and the fact that each impurity sees a different local density of states may give rise to non-Fermi-liquid signatures in the metal-insulator transition [7]. In quantum point contacts, Friedel oscillations associated with the proximity of a boundary lead to a coupling between the magnetic impurity and the electron gas which depends on both the position of the impurity and the energy of the electron state; as a consequence fluctuations of the Kondo properties are observed [8].

For closed systems, on the other hand, it is natural to ask: What is the effect of the confinement on the many-body physics? In ultra-small metal particles [2], for instance, the mean single-particle level

© EDP Sciences

spacing Δ can be comparable to the bulk Kondo temperature T_K^0. Clearly, a magnetic impurity in such a particle will show new physical properties associated with the new scale Δ produced by confinement. This has been studied theoretically in both metallic [9] and semiconductor heterostructure [10, 11] systems. However, most of these studies have neglected the *fluctuations* that are inherent in any mesoscopic sample (see however [12, 13]). Indeed, if Δ is the microscopic scale induced by the confinement, this latter brings in yet another energy scale, the Thouless energy $E_{\rm Th} \simeq \hbar/t_{\rm f}$ where $t_{\rm f}$ is the time to cross the nanostructure. The range of energy between Δ and $E_{\rm Th}$ is what is referred to as the mesoscopic regime. For a magnetic impurity coupled to electrons confined in a fully coherent nanoparticle at temperatures within this mesoscopic range, both the energies and the wave functions will display mesoscopic fluctuations which are stronger than those in open systems.

The goal of this study is to understand the effect of these mesoscopic fluctuations on the bulk universal behavior. Experimentally, our work bears on two situations: first, an ultra-small metallic particle [2] containing a single magnetic impurity, and, second, the tunable Kondo impurities that have been formed using quantum dots [14, 15]. We return in particular to the latter at the end of the paper. Our approach is to combine analytic renormalization analysis [8] with exact numerical results. The combination allows a quantitative understanding for $T \geq T_K^0$.

To describe a magnetic impurity coupled to a band of confined electrons, we start with the single-particle electron states ϵ_α and wave functions $\phi_\alpha(\mathbf{r})$ in the absence of the impurity. The impurity is modeled as a localized state at $\mathbf{r}=0$ with onsite repulsion U. Finally, there is hybridization between the impurity state c_d and electron states c_α; for a δ-like interaction, the electron gas is completely described by the local density of states (LDOS) $\rho_{\rm loc}(\epsilon) = \sum_\alpha |\phi_\alpha(0)|^2 \delta(\epsilon - \epsilon_\alpha)$.

The combination of electron states that is most localized on the impurity is $\psi_\sigma(0) = \sum_\alpha \phi_\alpha(0) c_{\alpha\sigma}$. The impurity couples to only this state of the electron gas. With locality and $SU(2)$ symmetry, the simplest model is a symmetric (i.e. $\epsilon_d = -U/2$) Anderson model,

$$H_{\rm And} = H_{\rm band} + H_{\rm imp} + V \sum_{\alpha\sigma} [\phi_\alpha^*(0) c_{\alpha\sigma}^\dagger c_{d\sigma} + {\rm h.c.}] \tag{1}$$

with $H_{\rm band} = \sum_{\alpha,\sigma} \epsilon_\alpha c_{\alpha\sigma}^\dagger c_{\alpha\sigma}$ and $H_{\rm imp} = \sum_\sigma \epsilon_d c_{d\sigma}^\dagger c_{d\sigma} + U n_{d\uparrow} n_{d\downarrow}$. We always take U large enough so that (1) is related through a Schrieffer-Wolff transformation to the Kondo model

$$H_{\rm Kondo} = H_{\rm band} + \sum_{\alpha\beta} J_{\alpha\beta} \overrightarrow{S} \cdot c_{\alpha\sigma_1}^\dagger \overrightarrow{\sigma}_{\sigma_1\sigma_2} c_{\beta\sigma_2} \tag{2}$$

where $J_{\alpha\beta} = J \phi_\alpha^*(0) \phi_\beta(0)$ and $J = 8V^2/U$. The band in the Kondo model must be cut at an energy scale $D_{\rm cut}$. ($D_{\rm cut} = 0.18\,U$ for the symmetric Anderson model [16, 17].) Numerical calculations will be performed with the Anderson Hamiltonian Eq. (1), but most of our discussion will involve the Kondo form (2).

Our goal here is to understand the fluctuations in measured quantities as the realization of the $\phi_\alpha(0)$ and ϵ_α changes. We focus on the case of chaotic confinement, for which a random matrix theory (RMT) description of the one-body physics is valid. For definiteness, we study the local susceptibility,

$$\chi = \int_0^\beta d\tau \langle {S_z}^d(\tau) {S_z}^d(0) \rangle \tag{3}$$

where ${S_z}^d(\tau) = e^{\tau H} \frac{1}{2}(n_{d\uparrow} - n_{d\downarrow}) e^{-\tau H}$. Experimentally, while this quantity is inaccessible for magnetic impurities, we indicate in our concluding discussion how to measure χ directly using quantum dots. In addition, most of our analysis and conclusions can be extended to other properties. In the absence of mesoscopic fluctuations (ϵ_α equally spaced and $\phi_\alpha = {\rm const.}$) and in the regime $\Delta \ll T \ll U$, χ shows universal behavior [4]: $T\chi = f(T/T_K^0)$ so that the energy scale T_K^0 is the only parameter.

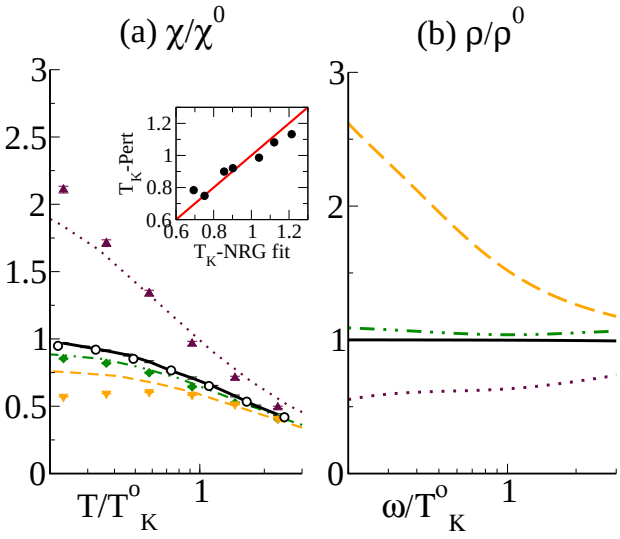

Fig. 1 – (a) QMC data for the local susceptibility of the Anderson model for the bulk-like case (open symbols) and three realizations of a mesoscopic electron sea (filled symbols). Also shown are the corresponding universal curves $\chi = f(T/T_K)/T$ for a realization dependent T_K obtained from Eq. (7) (the correspondence between symbols and lines is the natural one). Inset: for realisations for which a good fit with a universal curve is obtained, comparison of the $T_K^{\rm NRG}$ extracted from this fit , with the $T_K^{\rm pert}$ from perturbation theory [Eq. (7)]. (b) The smoothed local density of states at the impurity site for the same three realizations and the bulk case [line style matches the corresponding universal curves in (a)]. Note the striking non-universal curves for certain realizations and the correlation with variations in the density of states. The parameters are: $\Gamma \equiv \pi V^2/\Delta = 125\Delta, U = 250\Delta$. T is scaled to the corresponding bulk Kondo temperature $T_K^0 \simeq 10.2\Delta$ (value from Bethe ansatz). The realization dependent ϕ_α and ϵ_α are drawn from RMT-GOE and for the bulk case are $\phi_\alpha = 1$ with ϵ_α equally spaced.

Numerics. – Before turning to an analysis of the Hamiltonian Eq. (2) using the "poor man's scaling" technique [18], we present exact numerical data of χ for specific realizations of the closely related Hamiltonian Eq. (1). A key point is that the non-perturbative numerical data enables us to *quantitatively verify* that the perturbative "scaling" approach is sufficient to capture many aspects of the mesoscopic fluctuations, as well as to comment on the effect of these fluctuations in the low temperature regime where perturbation-theory is not valid. To get a non-perturbative hold on the Hamiltonian Eq. (1), we use a Quantum Monte-Carlo (QMC) method due to Hirsch and Fye [19]. Because only the d-site in the Anderson model is interacting, the introduction of one auxiliary bosonic variable renders the entire action quadratic in the fermionic fields. Integrating out the fermions leaves a determinant which is a functional of the bosonic variable. Finally, using the determinant as the weight to do importance sampling of the bosonic configuration, one can calculate imaginary time correlators of the Anderson model. We will study the correlator χ defined in Eq. (3).

Fig. 1(a) shows $\chi(T)$ for four different realizations of the conduction electron sea. The first one (open symbols) corresponds to the "bulk-like" case, by which we mean a discrete spectrum but without mesoscopic fluctuations (constant spacing of the energy levels, no fluctuations of the wave functions). The perfect agreement with the universal curve demonstrates that, at the temperature we consider, the discreetness of the spectrum per se plays no role.([1]) For the three remaining curves (filled symbols),

([1])This implies the absence of any even-odd effects such as the ones observed in [9], as well as any difference between the grand canonical and canonical ensembles. At lower T such effects would appear and could be captured by QMC techniques.

the one-body matrix describing the conduction electron Hamiltonian is drawn from the Gaussian orthogonal ensemble (GOE), which in particular implies independent Porter-Thomas distributions for the intensities $|\phi_\alpha(0)|^2$. Implicit here is the assumption that $E_{\rm Th} \to \infty$, which, as discussed below, is a well-defined limit in the chaotic case.

An important result arising from these calculations is that not all of the QMC data can be described by the universal form, $\chi = f(T/T_K)/T$, with a realization dependent T_K. This is particularly evident in cases in which χ turns down at low-T since $f(T/T_K)/T$ is a monotonically decreasing function. A more detailed analysis shows that for the parameters used in Fig. 1, only about half of the realizations yield a temperature dependent susceptibility that can be scaled onto the universal curve with reasonably good accuracy. *Clearly, mesoscopic fluctuations can cause significant deviations from universality*.

Poor Man's Scaling. – The basic idea of this technique is that Hamiltonian H with bandwidth $D_{\rm cut}$ can be replaced with another Hamiltonian H' with smaller bandwidth while keeping the low energy physics unchanged. In the bulk case, the only coupling parameter is $J\rho_0$, and its "renormalization" causes it to diverge as the bandwidth approaches an energy scale that may be identified with T_K^0. In our case of a discrete spectrum, we take out a single level at a time. Following Anderson, upon removing the topmost level ϕ_β, in order to keep low energy physics unchanged, the amplitude $J_{\alpha\gamma}$ between two low energy states changes by $\delta J_{\alpha\gamma} = J_{\alpha\beta}J_{\beta\gamma}/\epsilon_\beta$. Interestingly, this equation is solved by $\delta J_{\alpha\gamma}$ of the form $(\delta J)\phi^*_\alpha(0)\phi_\gamma(0)$ with

$$\delta J = J^2 \frac{|\phi_\beta(0)|^2}{\epsilon_\beta}\,, \quad \frac{\delta J}{\delta D} = J^2 \frac{\rho_{\rm loc}(D)}{D}\,. \tag{4}$$

Thus in the "poor man's scaling" approach, the effect of reducing D is captured by letting J flow, obtaining at low temperature T the effective coupling constant

$$J_{\rm eff}(T) \simeq \frac{J}{1 - J\int_T^{D_{\rm cut}} \rho_{\rm loc}(\epsilon)d\epsilon/\epsilon}\,, \tag{5}$$

where J is the "bare" coupling constant defined at the cutoff of the Kondo model Eq. (2). In the bulk problem it is well known that the "poor man's scaling" result can also be reproduced by two other perturbative approaches, namely a one-loop renormalization group analysis, and Abrikosov's method for resumming the "parquet" diagrams [20]. This is also true in the presence of fluctuations (see e.g. [8] in the perturbative renormalization group context). By working at finite temperature (using Matsubara Green functions in conjunction with the other perturbative approaches) $\rho_{\rm loc}(\epsilon)$ in Eq. (5) is replaced by a more natural smoothed LDOS

$$\rho_{\rm sm}(\omega) = \frac{\omega}{\pi}\int_{-\infty}^{\infty} d\epsilon \frac{\rho_{\rm loc}(\epsilon)}{\omega^2 + \epsilon^2}, \tag{6}$$

In the following we shall discuss our results in terms of the smoothed LDOS Eq. (6). We note that one-loop RG analysis has been shown to be a controlled approximation only for a flat (bulk) density of states; hence, for the mesoscopic regime, we turn to a comparison with the exact numerics.

Comparison of Numerics with Poor Man's Scaling. – At a qualitative level, the relevance of $\rho_{\rm sm}(\omega)$ can be assessed by comparing panels (a) and (b) of Fig. 1, where we have plotted the functions $\chi(T)$ and $\rho_{\rm sm}(\omega)$ for the same realizations. Note that the cases with large deviations from the universal behavior are those for which $\rho_{\rm sm}$ changes the most from the high to low energy scales. The non-monotonic behavior of χ for one realization may be understood as being due to a peak in $\rho_{\rm sm}$ at low frequencies. In other cases a dip in $\rho_{\rm sm}$ causes χ to increase continuously, perhaps until $T \sim \Delta$. In such cases there is no "Fermi-liquid" regime ($\chi \sim$ constant and $T > \Delta$) even though the bulk case has such a regime.

As the Kondo temperature is defined as the scale at which the effective coupling constant $J_{\rm eff}$ diverges, it is natural to evaluate the realization dependent *fluctuations* of T_K around the bulk value T_K^0 using the perturbative Kondo temperature $T_K^{\rm pert}$ defined as

$$\int_{T_K^{\rm pert}}^{D_{\rm cut}} \rho_{\rm sm}(\omega)\frac{d\omega}{\omega} = \int_{T_K^0}^{D_{\rm cut}} \overline{\rho}_{\rm sm}(\omega)\frac{d\omega}{\omega} \ , \tag{7}$$

where $\overline{\rho}_{\rm sm}$ is averaged over realizations and so is by construction essentially constant. The lines in Fig. 1(a) correspond to the universal curves $\chi(T) = f(T/T_K^{\rm pert})/T$. Clearly, the high temperature (i.e. above $T_K^{\rm pert}$) part of the QMC data is well described in this way. To evaluate how quantitatively Eq. (7) describes the data, we furthermore consider *all* our realisations that show approximately "universal" behavior, in the sense that the data follow the bulk universal curve obtained from NRG rescaled with an appropriate fitted Kondo temperature. This constitutes approximately two-thirds of the realisations studied. We have then compared (inset in Fig. 1) this $T_K^{\rm NRG}$ *fit* with the energy scale $T_K^{\rm pert}$ given by Eq. (7). The agreement is quite good, especially considering that Eq. (7) is meant to define an energy scale rather than an exact number.

It has to be borne in mind, however, that with the Hirsch and Fye algorithm we are using, the ratio U/T that can be practically investigated cannot be made much larger than 500. The parameters used in Fig. 1 have been chosen in such a way that temperature significantly smaller than the bulk Kondo temperature T_K^0 can be reached, so that the absence of scaling behavior in the low temperature regime could be demonstrated. This however means that $D_{\rm cut} \equiv 0.18U \simeq 16.6T_K^0$ is only a little bit more than a decade larger than the bulk Kondo temperature. Here this implies that a good part of the fluctuations seen in the high temperature part of Fig. 1 could be explained by fluctuations of the smooth density of states $\rho_{\rm sm}$ *at* $D_{\rm cut}$.

To show that the one-loop renormalization analysis indeed captures the fluctuations associated with the energy dependence of the density of states, we have performed another set of QMC simulations, with the parameters $\Gamma = 250\Delta$ and $U = 1000\Delta$, so that $D_{\rm cut} = 180\Delta$ and $T_K^0 \simeq 5.1\Delta$. The larger value of $D_{\rm cut}$ already implies that $\rho_{\rm sm}(D_{\rm cut})$ shows significantly less fluctuations. To completely exclude the possibility that the observed fluctuation of the susceptibility is an effect of variations of the smooth density of states at the scale $D_{\rm cut}$, we furthermore *rescale* all the density of states [i.e. multiply the $\phi_\alpha(0)$ by a constant] so that $\rho_{\rm sm}(D_{\rm cut}) = \rho_0$ for all realizations. The resulting temperature dependent susceptibility, for four realizations (selected because they display large density of states fluctuations), is shown in Fig. 2. The comparison with the universal curves $f(T/T_K^{\rm pert})/T$ shows that in this case, also, the high temperature part of the QMC data is well described in this way. It is particularly remarkable, in both Figs. 1 and 2, that the RG result works for temperatures as low as T_K or even below.

We thus reach the central result of this paper: *The excellent agreement seen in Fig. 2 between theoretical predictions obtained in this way and exact numerical calculations provides a numerical demonstration that this approach is a sound starting point for including mesoscopic fluctuations.*

Fluctuations of T_K. – This agreement justifies using $T_K^{\rm pert}$ as the crossover temperature from weak to strong coupling, even for realisations for which the universal scaling is destroyed by the mesoscopic fluctuations. Within our RMT modeling, the variance of $T_K^{\rm pert}$ can be easily evaluated from Eq. (7) in the limit $\delta T_K = (T_K^{\rm pert} - T_K^0) \ll T_K^0$ as [21]

$$\frac{\langle \delta {T_K}^2 \rangle}{{T_K^0}^2} \simeq \alpha \frac{\Delta}{T_K^0} \ . \tag{8}$$

For our model, $\alpha = (4/\pi)\ln 2$; more generally it is a number of order 1. An improved model can be developed through semiclassical analysis, in which case $\langle\cdot\rangle$ may signify an energy average. The

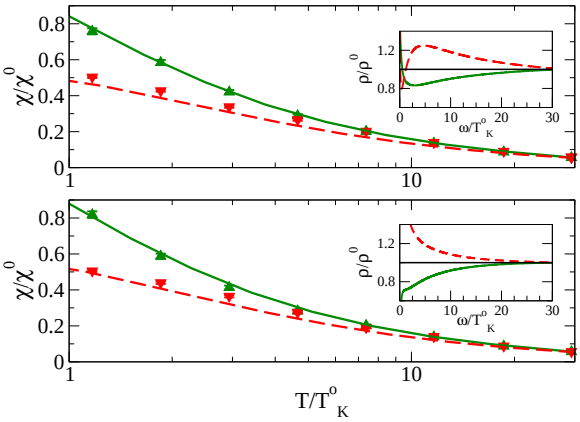

Fig. 2 – Triangles: QMC calculation of the local susceptibility for four realizations, with the parameters $\Gamma = 250\Delta$ and $U = 1000\Delta$, so that $D_{\rm cut} = 180\Delta \simeq 35.3T_K^0$, with $T_K^0 \simeq 5.1\Delta$. Lines: universal curves using $T_K^{\rm pert}$ from Eq. (7). Inset: Corresponding smoothed densities of states (with matching line styles).

correlator $\langle \rho_{\rm sm}(\omega)\rho_{\rm sm}(\omega')\rangle$ is then related to the Fourier transform of the classical probability $P_{\rm cl}(t)$ that a particle starts at the impurity with energy E_F and returns there after time t [22]. Eq. (8) can therefore be generalized to

$$\frac{\langle \delta {T_K}^2 \rangle}{{T_K^0}^2} \simeq \frac{2\Delta V}{\pi\hbar} \int_{T_K^0}^{D_{\rm cut}} \frac{d\omega_1'}{\omega_1'} \frac{d\omega_2'}{\omega_2'} \int_0^\infty dt P_{\rm cl}(t) e^{-(\omega_1'+\omega_2')t/\hbar} \tag{9}$$

(V is the volume of the dot). For chaotic systems,

$$\begin{aligned} P_{\rm cl}(t) &= 0 \qquad \text{for } \; t < \hbar/E_{\rm Th} \\ P_{\rm cl}(t) &= 1/V \qquad \text{for } \; t > \hbar/E_{\rm Th} \end{aligned} \tag{10}$$

so that Eq. (8) is then trivially recovered in the limit $y \equiv E_{\rm Th}/T_K^0 \to \infty$. The fluctuations of T_K vanish, of course, in the opposite limit $y \to 0$. A remarkable implication of Eqs. (9)-(10) is that the value of $E_{\rm Th}$ does not affect the mesoscopic fluctuations for a chaotic system with $E_{\rm Th} \gg T_K$. The fluctuations are in this sense "universal", and are described by RMT for any chaotic system.

Conclusions. – We have shown that the mesoscopic fluctuations typical in nanostructures significantly affect the physics of a Kondo impurity. Our main result is a demonstration that the *fluctuations* of the high temperature properties can be understood by following a simple poor man's scaling argument (or, equivalently, one-loop RG or resummation of parquet diagrams) and that this works down to $T \approx T_K$. In addition, we show (1) deviations from universal behavior at low temperature, (2) an explicit formula for the variance of the Kondo temperature, and (3) a semiclassical connection between the fluctuations of T_K and the classical probability of return.

Kondo physics has recently received renewed attention because of its relevance to the low temperature physics of quantum dots [14, 15]. These "artificial magnetic impurities" provide tunability of the microscopic Hamiltonian, and can be naturally interfaced with larger quantum dots displaying the kind of mesoscopic fluctuations that we address here. From an experimental point of view, the physics we are discussing should be easily observable in such systems. In particular, we stress that though we have here specifically considered the local susceptibility, the qualitative features we have discussed – the mere existence of the mesoscopic fluctuations, the absence of universality of the low

temperature regime, and the universal character, but with a realisation dependent Kondo temperature, of the $T \geq T_K$ regime – should be observed for other physical quantities. In the same way, the fact that the the realisation dependent Kondo temperature can be extracted from a fit to the universal form in the high temperature regime implies that our quantitative predictions Eqs. (8)-(9) can also be tested on physical quantities other than the local susceptibility.

Finally, we mention that experimental set-ups where the correlator Eq. (3) can be directly measured are also possible. In particular, the problem of charge fluctuations in a gated, Coulomb blockaded metal grain [23] has been shown to be equivalent to a Kondo problem [24]. In this mapping the charge and gate voltage of the CB problem map to the spin of the Kondo impurity and a *local* magnetic field applied to it. The differential capacitance at a degeneracy point in the CB problem is thus equivalent to the *local* susceptibility Eq. (3) of a Kondo problem. In the presence of a strong polarizing magnetic field, the equivalent Kondo Problem is described by exactly our Hamiltonian Eq. (2). Thus, a gated dot connected to another dot provides a realization of a Kondo impurity coupled to a mesoscopic electron gas where it is possible to measure the correlator Eq. (3) directly.

* * *

It is a pleasure to thank P. Brouwer, A. Finkelstein, L. Glazman, C. Marcus, K. Matveev, M. Vojta, and J. Yoo for valuable discussions. This work was supported in part by the NSF (DMR-0103003).

REFERENCES

[1] ALEINER I. L., BROUWER P. W. and GLAZMAN L. I., *Phys. Rep.*, **358** (2002) 309 and references therein.
[2] VON DELFT J. and RALPH D. C., *Phys. Rep.*, **345** (2001) 61
[3] FISHER M. P. A. and GLAZMAN L. I., *Mesoscopic Electron Transport*, edited by L. L. SOHN, L. P. KOUWENHOVEN, and G. SCHÖN (Kluwer Academic Publishers) 1997, p. 331
[4] A. C. HEWSON, *The Kondo Problem to Heavy Fermions*. (Cambrige University Press) 1993
[5] OKHAWA F. J., FUKUYAMA H. and YOSIDA K., *Journal of the Physical Society of Japan*, **52** (1983) 1701
[6] MARTIN I., WAN Y. and PHILLIPS P., *Phys. Rev. Lett.*, **78** (1997) 114
[7] DOBROSAVLJEVIC V., KIRKPATRICK T. R. and KOTLIAR. G., *Phys. Rev. Lett.*, **69** (1992) 1113
[8] ZARÁND G. and UVARDI L., *Phys. Rev. B*, **54** (1996) 7606
[9] THIMM W. B., KROHA J. and VON DELFT J., *Phys. Rev. Lett.*, **82** (1999) 2143
[10] SIMON P. and AFFLECK I., *Phys. Rev. Lett.*, **89** (2002) 206602
[11] CORNAGLIA P. S. and BALSEIRO C. A., *Phys. Rev. Lett.*, **90** (2003) 216801
[12] KAUL R. K., ULLMO D. and BARANGER H. U., *Phys. Rev. B*, **68** (2003) 161305(R)
[13] LEWENKOPF C. H. and WEIDENMULLER H. A., *Phys. Rev. B*, **71** (2005) 121309
[14] GOLDHABER-GORDON D., SHTRIKTMAN H., MAHALU D., ABUSCH-MAGDER D., MEIRAV U. and KASTNER M. A.,. *Nature*, **391** (1998) 156
[15] PUSTILNIK M., GLAZMAN L. I., COBDEN D. H. and KOUWENHOVEN L. P., Lecture Notes in Physics, Vol. **3**, p. 579 2001
[16] HALDANE F. D. M., *J. Phys. C: Solid State Phys.*, **11** (1978) 5015
[17] WILSON K. G., *Rev. Mod. Phys.*, **47** (1975) 773
[18] ANDERSON P. W., *J. Phys. Chem.*, **3** (1970) 2346
[19] HIRSCH J. E. and FYE R. M., *Phys. Rev. Lett.*, **56** (1986) 2521
[20] ABRIKOSOV A. A., *Physica (Utrecht)*, **2** (1965) 5
[21] A similar result has been obtained independently by S. Kettemann, cond-mat/0409417.
[22] ARGAMAN N., IMRY Y. and SMILANSKY U., *Phys. Rev. B*, **47** (1993) 4440
[23] BERMAN D., ZHITENEV N. B., ASHOORI R. C. and SHAYEGAN M., *Phys. Rev. Lett.*, **82** (1999) 161 and references therein.
[24] MATVEEV K. A., *Sov. Phys. JETP*, **72** (1991) 892